Report

Cell Reports

α/β-Hydrolase Domain 6 in the Ventromedial Hypothalamus Controls Energy Metabolism Flexibility

Graphical Abstract

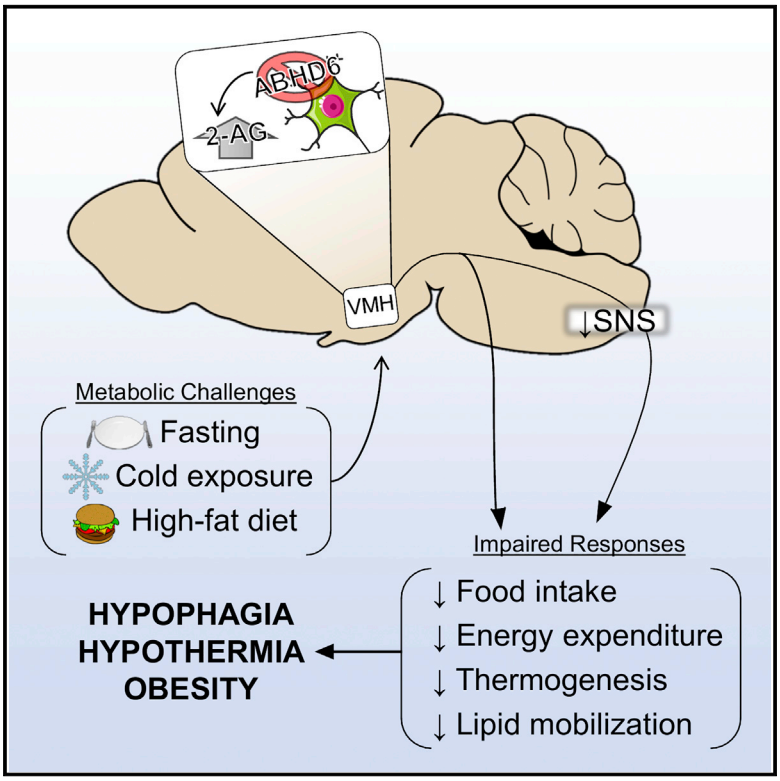

Authors

Alexandre Fisette, Stephanie Tobin, Léa Décarie-Spain, ..., Marc Prentki, Stephanie Fulton, Thierry Alquier

Correspondence

stephanie.fulton@umontreal.ca (S.F.), thierry.alquier@umontreal.ca (T.A.)

In Brief

Fisette et al. demonstrate that the endocannabinoid-degrading enzyme ABHD6 in ventromedial hypothalamus neurons is a regulator of VMH 2-AG accumulation and energy metabolism flexibility in response to homeostatic challenges. ABHD6 knockout in VMH neurons of adult mice impairs the feeding response to fasting and increases susceptibility to cold-induced hypothermia, diet-induced obesity, and resistance to diet-induced weight loss.

Highlights

- VMH neuronal ABHD6 deletion blunts fasting-induced feeding in a 2-AG-dependent manner
- ABHD6 loss-of-function in VMH neurons impairs cold-induced thermogenesis
- ABHD6 VMH knockout reduces adaptive thermogenesis and enhances diet-induced obesity
- ABHD6 in the VMH promotes resistance to dieting and defense of body weight

Fisette et al., 2016, Cell Reports *17*, 1217–1226
October 25, 2016
http://dx.doi.org/10.1016/j.celrep.2016.10.004

Cell Reports
Report

α/β-Hydrolase Domain 6 in the Ventromedial Hypothalamus Controls Energy Metabolism Flexibility

Alexandre Fisette,[1,2] Stephanie Tobin,[1,2] Léa Décarie-Spain,[1,3] Khalil Bouyakdan,[1,4] Marie-Line Peyot,[1] S.R. Murthy Madiraju,[1] Marc Prentki,[1,2,4] Stephanie Fulton,[1,2,*] and Thierry Alquier[1,4,5,6,*]
[1]CRCHUM and Montreal Diabetes Research Center
[2]Department of Nutrition
[3]Department of Neuroscience
[4]Department of Biochemistry and Molecular Medicine
[5]Department of Medicine
Université de Montréal, Montreal, QC H3T1J4, Canada
[6]Lead Contact
*Correspondence: stephanie.fulton@umontreal.ca (S.F.), thierry.alquier@umontreal.ca (T.A.)
http://dx.doi.org/10.1016/j.celrep.2016.10.004

SUMMARY

α/β-Hydrolase domain 6 (ABHD6) is a monoacylglycerol hydrolase that degrades the endocannabinoid 2-arachidonoylglycerol (2-AG). Although complete or peripheral ABHD6 loss of function is protective against diet-induced obesity and insulin resistance, the role of ABHD6 in the central control of energy balance is unknown. Using a viral-mediated knockout approach, targeted endocannabinoid measures, and pharmacology, we discovered that mice lacking ABHD6 from neurons of the ventromedial hypothalamus (VMH^{KO}) have higher VMH 2-AG levels in conditions of endocannabinoid recruitment and fail to physiologically adapt to key metabolic challenges. VMH^{KO} mice exhibited blunted fasting-induced feeding and reduced food intake, energy expenditure, and adaptive thermogenesis in response to cold exposure, high-fat feeding, and dieting (transition to a low-fat diet). Our findings identify ABHD6 as a regulator of the counter-regulatory responses to major metabolic shifts, including fasting, nutrient excess, cold, and dieting, thereby highlighting the importance of ABHD6 in the VMH in mediating energy metabolism flexibility.

INTRODUCTION

Metabolic and behavioral processes adjust to changing environmental conditions, including variations in the availability of food and its composition. This flexible nature of energy metabolism is fundamental to homeostatic regulation commanded by hypothalamic nuclei. Consistent with a neuromodulatory role, endocannabinoids have the capacity to dynamically alter neurotransmission in a manner specialized to the neuronal population affected and are thus well-suited to generating on-demand metabolic adaptations to changing energy needs. The endocannabinoid system (ECS) plays an important role in hypothalamic control of energy balance (Busquets-Garcia et al., 2015). A consequence of increased ECS activity in the hypothalamus is stimulation of food intake, with concomitant energy sparing.

The most abundant brain endocannabinoid, 2-arachidonoylglycerol (2-AG), is synthesized postsynaptically upon neuronal activation and exerts most of its effects by retrograde signaling via presynaptic CB1 receptors (CB1Rs). The enzymes responsible for endocannabinoid synthesis and degradation can profoundly affect the net outcome of ECS activation. 2-AG is classically described as degraded by monoacylglycerol lipase (MAGL) in the presynaptic neuron. However, the recently discovered serine hydrolase α/β-hydrolase domain 6 (ABHD6) degrades 2-AG directly at the site of its synthesis, ultimately affecting 2-AG levels and action at CB1R (Blankman et al., 2007; Marrs et al., 2010). Pharmacological inhibition of ABHD6, leading to elevated brain 2-AG levels, is beneficial for autoimmune encephalomyelitis (Wen et al., 2015) and epilepsy (Naydenov et al., 2014), yet the contribution of ABHD6 to the central control of energy metabolism is unknown. Whole-body or peripheral knockout or knockdown of ABHD6 demonstrates strong therapeutic potential for ABHD6 inhibition, with respect to insulin secretion (Zhao et al., 2014, 2015), as well as insulin sensitivity and obesity (Zhao et al., 2016). These mice are resistant to diet-induced obesity (Thomas et al., 2013; Zhao et al., 2016) and exhibit improved glucose tolerance and insulin sensitivity, partly explained via enhanced brown adipose tissue activation and white adipose browning (Zhao et al., 2016).

The ECS plays an important role in the control of feeding and energy expenditure by the ventromedial hypothalamus (VMH) (Busquets-Garcia et al., 2015). CB1R is strongly expressed in neurons of the VMH (Marsicano and Lutz, 1999), and deletion of CB1R in steroidogenic factor 1 (SF1) neurons of the VMH increases insulin sensitivity and thermogenesis in chow-fed mice, yet surprisingly increases susceptibility to diet-induced obesity in high-fat-fed mice (Cardinal et al., 2014). Despite these findings, the impact of elevated endogenous levels of 2-AG in the

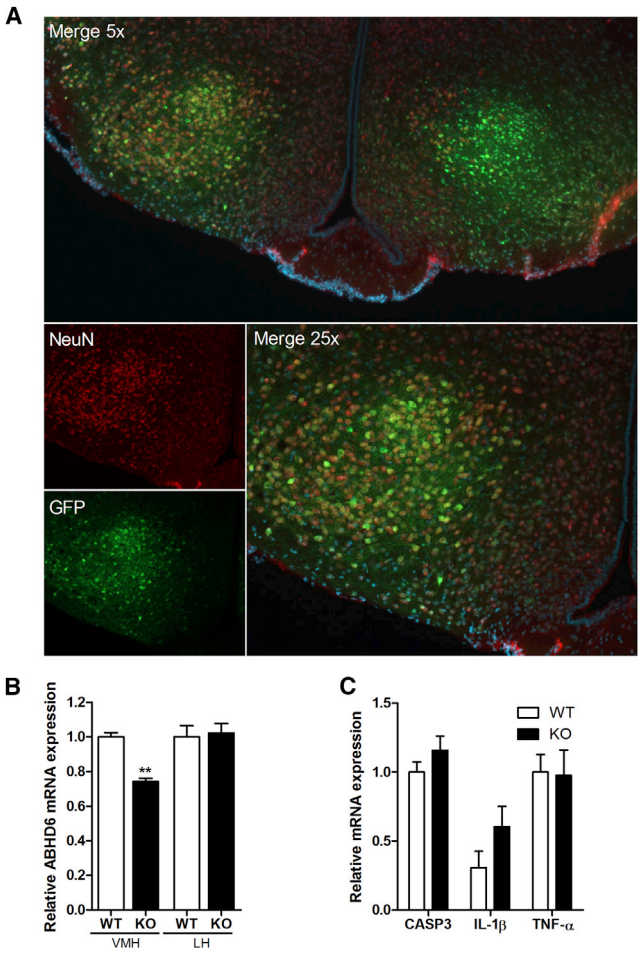

Figure 1. Validation of ABHD6 Loss-of-Function in VMH Neurons

(A) Visualization of neurons (red) using neuronal nuclei (NeuN) marker, GFP (green), and Merge (orange) in floxed mice injected with AAV2/1.hSynap.HI.GFP.CreWPRE.SV40. Nuclei are stained in blue using 4,6-diamidino-2-phenylindole staining (DAPI).

(B) Expression of *ABHD6* in the VMH and LH corrected by *β-actin* and normalized to the respective WT region.

(C) Unaltered relative expression of mRNA markers of inflammation and apoptosis in the VMH of VMH^{KO} mice. All results are expressed as mean ± SEM. n = 7.

VMH and the role of ABHD6 in the control of energy balance is unknown. To this end, we used a viral strategy to knockout ABHD6 from VMH neurons of adult mice. ABHD6 deletion in VMH neurons impairs the counter-regulatory response to key metabolic challenges, including fasting-induced feeding, diet-induced obesity, dieting (transition to a low-fat diet), and cold-induced thermogenesis, thereby highlighting the importance of ABHD6 in the VMH in adapting to changing energy demands.

RESULTS AND DISCUSSION

Neuronal ABHD6 Loss-of-Function in the VMH

To determine the impact of neuron-specific ABHD6 in the VMH, a conditional loss-of-function approach was used, whereby adeno-associated viruses (AAVs) expressing Cre or GFP under the control of the synapsin promoter were microinjected into the bilateral VMH of adult ABHD6-floxed mice. AAV injection location, spread, and neuronal specificity was confirmed by histology and immunohistochemistry (Figure 1A). *ABHD6* expression in the VMH is comparable to other hypothalamic nuclei (Figure S1A) and was reduced by an average of 26% ($p < 0.01$) in mice receiving AAV-Cre ("VMH^{KO}") relative to controls ("VMH^{WT}"), whereas it was unchanged in the neighboring lateral hypothalamus (Figure 1B). Cell counts showed that 84 ± 4% of VMH NeuN-positive cells were GFP positive. No sign of inflammation or apoptosis was detected in VMH knockout (VMH^{KO}) versus VMH wild-type (VMH^{WT}) (Figure 1C). In view of evidence that *ABHD6* is also expressed in astrocytes (Marrs et al., 2010), the relatively modest reduction in *ABHD6* mRNA may be largely attributed to the neuronal specificity of the knockout because NeuN-positive cells represented only 60 ± 4% of all VMH cells.

Disruption of ABHD6 in the VMH Alters Fasting Refeeding Via Elevated 2-AG

We next sought to determine if ABHD6 loss of function in VMH neurons alters energy balance under basal conditions in chow-fed mice. Cumulative food intake was slightly elevated by the 12th week of measurement (+9%, $p < 0.05$), whereas body weight and feed efficiency were unchanged (Figures 2A–2C). Energy expenditure (Figures 2D and 2E) and respiratory exchange ratio (RER) (Figures S2A and S2B) remained similar between free-feeding VMH^{KO} and VMH^{WT} mice. There was a trend toward lower movement during the dark phase ($p = 0.08$) (Figures 2F and 2G), an observation not tied to altered anxiety-like behavior (Figure S1B). Echo MRI revealed a trend for increased total fat mass ($p = 0.07$), with no change in lean mass (Figure S1C). Both subcutaneous inguinal ($p = 0.05$) and visceral epididymal ($p = 0.08$) fat depot weights were elevated in VMH^{KO} mice (Figure S1D). Glucose tolerance was unchanged (Figure S2E).

The absence of major differences in food intake (Figure 2A) is not surprising in light of reports that disruption of CB1R signaling via pharmacological blockade or gene knockout inhibits food intake only in response to fasting (Di Marzo et al., 2001). Accordingly, we next sought to investigate food intake following varying fast lengths, ranging from 0 to 18 hr (Figure 2H). Food intake in response to a 4-hr and 18-hr fast was diminished in VMH^{KO} mice as compared to VMH^{WT} mice (4-hr fast, −30%, $p < 0.05$; 18-hr fast, −25%, $p < 0.05$). No significant changes were detected in nonfasted (0 hr) or 2-hr-fasted conditions (+23%, $p = 0.1$).

Endocannabinoids are well known to increase food intake, but this orexigenic effect can be abolished by excess CB1R activation. Indeed, endocannabinoids exert a biphasic control of food intake: low-to-moderate doses of 2-AG or the selective CB1R agonist arachidonyl-2-chloroethylamide increase food intake, whereas high concentrations can elicit anorectic actions (Bellocchio et al., 2010; Koch et al., 2015). Brain endocannabinoid levels are increased by 30%–100% during fasting (Hanus et al., 2003; Kirkham et al., 2002) and by 33%–80% with ABHD6 inhibition (Wen et al., 2015). Therefore, we posited that the blunted fasting-refeeding response we observed in VMH^{KO} mice might result

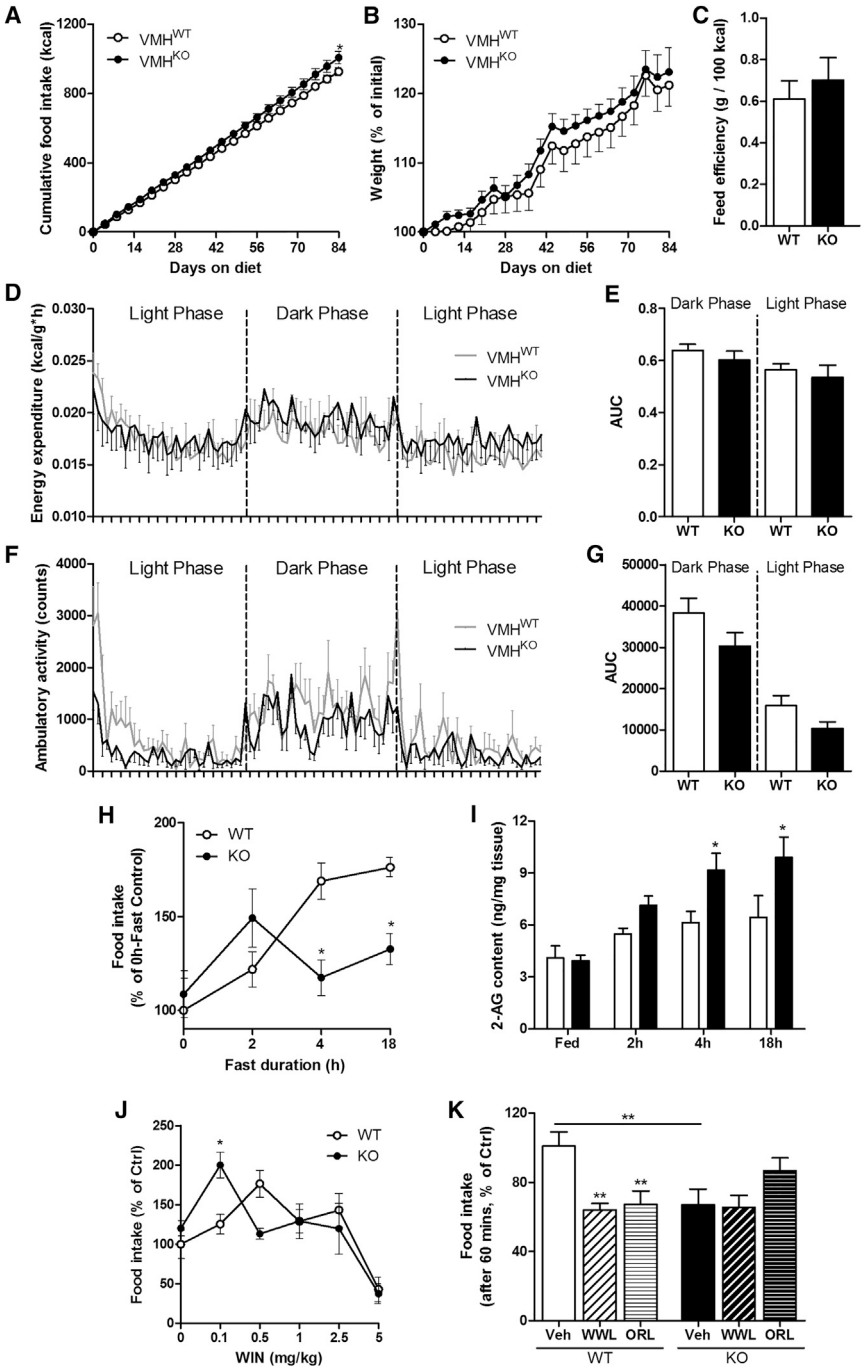

Figure 2. ABHD6 Loss of Function in VMH Neurons Suppresses Fasting Refeeding Via 2-AG

(A) Cumulative food intake (kcal).

(B) Body weight (% of initial weight).

(C) Feed efficiency (g of body weight gained/100 kcal of cumulative food intake).

(D) Energy expenditure over 36 hr corrected by metabolic mass (kcal/g*h).

(E) Area under the curve of the last dark and light phase of (D).

(F) Ambulatory activity.

(G) Area under the curve of the last dark and light phase of (F).

(H) Food intake 2 hr after refeeding decreases in VMH^{KO} mice, with fast lengths from 0 to 18 hr (% controls).

(I) Total VMH 2-AG content (ng 2-AG + 1-AG /mg of fresh tissue) is similar in fed and 2-hr-fasted groups, but increases in 4-hr- and 18-hr-fasted VMH^{KO} mice.

(J) Food intake 2 hr after injection of the CB1R agonist WIN55-212 (0–5 mg/kg) of 2-hr-fasted mice follows a biphasic curve that is shifted to the left in VMH^{KO} mice (% controls).

(K) Normalization of food intake 1 hr after refeeding of 4-hr-fasted mice treated in the VMH with orlistat (1.25 μg) or ABHD6 inhibitor WWL70 (1.0 μg) (% controls). All results are expressed as mean ± SEM, in which differences versus controls are expressed as $^*p < 0.05$; $^{**}p < 0.01$. n = 5–7 per group for (A–I and K). n = 9-10 for (J).

from higher than normal VMH ECS activity. To begin testing this hypothesis, we measured 2-AG content exclusively in the VMH under fed conditions and following varying degrees of fasting. Although no difference could be detected between groups under fed conditions, VMH^{KO} mice showed increased VMH 2-AG content relative to VMH^{WT} mice after a 4-hr or 18-hr fast (+50%, $p < 0.05$, and +54%, $p < 0.05$, respectively) (Figure 2I).

To further test the hypothesis that elevated levels of 2-AG in VMH^{KO} mice contributes to the reduced fasting-refeeding response, we assessed food intake in response to increasing doses of the CB1R agonist WIN55-212 (WIN) in 2-hr-fasted mice. We chose the 2-hr-fasting duration because VMH^{KO} mice exhibit a hyperphagic response comparable to VMH^{WT} in this condition (Figure 2H). In addition, based on measurements of VMH 2-AG levels, 2-AG content of the VMH^{KO} mice at this fast duration is slightly higher (+30%; Figure 2I) than that in VMH^{WT} mice, but not yet capable of attenuating the fasting-refeeding response (as shown in Figure 2H). As reported previously (Bellocchio et al., 2010; Koch et al., 2015), we observed a biphasic response to CB1R agonism in VMH^{WT} mice: 0.1- and 0.5-mg/kg doses of WIN increased food by 25% and 76% ($p < 0.05$), respectively, whereas doses higher than 1.0 mg/kg failed to increase food intake (Figure 2J). In contrast, the dose-response curve shifted to the left in VMH^{KO} mice, such that a lower dose of WIN (0.1 mg/kg) elicited the greatest increase in food intake (+100%) and doses of 0.5 mg/kg and higher had no effect on feeding, which is reflective of the higher 2-AG content in the VMH at the time of the injections. Once again, these data suggest that high ECS activity in the VMH, as seen in VMH^{KO}

mice, can decrease the orexigenic effects of endocannabinoids in a CB1R-dependent manner. To further support this possibility, we pharmacologically halted 2-AG synthesis to determine if it normalizes fasting-refeeding responses between VMH^{KO} and VMH^{WT} mice. To this end, we infused orlistat, a blocker of 2-AG synthesis (diacylgycerol lipase [DAGL]/pan-lipase inhibitor), into the VMH. In addition, we set out to determine if we can recapitulate the feeding phenotype of VMH^{KO} mice with injections of an ABHD6 inhibitor (WWL70) into the VMH. As we found before (Figure 2H), VMH^{KO} animals consumed less food than VMH^{WT} animals after a 4-hr fast (vehicle injection, −33%, $p < 0.01$) (Figure 2K). Inhibiting 2-AG synthesis during the fast with orlistat inhibited food intake in VMH^{WT} mice, as expected (−39%, $p < 0.01$). Moreover, food intake following orlistat treatment was similar between VMH^{KO} and VMH^{WT}, thus blocking 2-AG synthesis normalized food intake between groups. On the other hand, pharmacological inhibition of ABHD6 in the VMH of VMH^{WT} mice recapitulated the feeding behavior of VMH^{KO} mice without affecting feeding in VMH^{KO} mice. This last experiment suggests that ABHD6 inhibition in *neurons* drives the fasting-refeeding phenotype. Collectively, we demonstrate that increasing 2-AG levels exclusively in the VMH via neuronal ABHD6 loss of function affects feeding and CB1R function. Although less likely, these effects could also be partially mediated via CB2R because both 2-AG and WIN can bind and activate CB2R. It is, however, still unclear if neurons, particularly in the hypothalamus, express CB2R. The biphasic effects of whole-brain CB1R activation on feeding have previously been linked with striatal CB1R (Bellocchio et al., 2010), whereas results here suggest that this effect also relies on the VMH.

Deletion of ABHD6 in the VMH Impairs Cold-Induced Thermogenesis

Endocannabinoids are well-known to modulate body temperature (Holtzman et al., 1969), and elevation of whole-brain 2-AG levels through MAGL inhibition has been shown to elicit a CB1R-mediated hypothermic response in mice during a cold challenge (Nass et al., 2015). Moreover, the VMH is implicated in the regulation of thermogenesis through activation of sympathetic nervous system (SNS) outputs (Kim et al., 2011). Thus, we next set out to examine the response to acute cold exposure using internal core temperature probes and indirect calorimetry. Although energy expenditure and body temperature at 22°C were similar, VMH^{KO} mice did not adapt to cold as well as VMH^{WT} mice did when exposed to a temperature of 10°C; VMH^{WT} mice increased their energy expenditure by 81% versus 65% for VMH^{KO} ($p < 0.001$ for both) (Figures 3A and 3B). Core body temperature dropped by 0.86°C for VMH^{WT} and by 1.14°C for VMH^{KO} ($p < 0.05$) (Figures 3C and 3D). Temperatures of 4°C differentially increased energy expenditure to 116% of basal for VMH^{WT} mice, but only to 86% of basal for VMH^{KO} ($p < 0.05$), and lowered core body temperature by 1.63°C for VMH^{WT} and by 2.13°C for VMH^{KO} versus basal (0.69°C difference; $p < 0.01$). Reflecting increased use of lipids as energy substrates, average RER for both VMH^{WT} and VMH^{KO} mice decreased with temperature ($p < 0.05$ for both groups at 4°C and 10°C); however, the average RER was significantly higher in VMH^{KO} at 4°C in comparison with VMH^{WT} ($p < 0.01$), which is indicative of reduced lipid oxidation at 4°C (Figures 3E and 3F).

We subsequently exposed a separate cohort of mice to 4°C for 24 hr and examined food intake, plasma lipids, and brown fat activity markers. Cumulative food intake over 24 hr was reduced in VMH^{KO} mice (−26%, $p < 0.05$) (Figure 3G). In line with the indirect calorimetry data, VMH^{KO} mice had a lower expression of brown fat *UCP1* (−39%, $p < 0.01$) and *PGC1-α* (−47%, $p < 0.01$) and reduced plasma nonesterified fatty acids (NEFAs) (−33%, $p < 0.05$) (Figures 3H and 3I). These results suggest that VMH ABHD6 contributes to the counter-regulatory response to cold exposure, likely via an endocannabinoid-dependent mechanism that regulates food intake, lipid mobilization, and brown fat thermogenesis. Based on these findings and the role of ECS in thermoregulation via sympathetic outputs, the phenotype of cold-exposed VMH^{KO} mice is likely due to increased VMH ECS activity and reduced SNS outflow.

VMH^{KO} Mice Exhibit Reduced Adaptive Thermogenesis and Are Prone to Diet-Induced Obesity

Hypothalamic 2-AG content doubles when mice are placed on a high-fat (HF) diet for more than 2 weeks (Higuchi et al., 2012). This rise in hypothalamic 2-AG is believed to play a role in the development of obesity because it reduces energy expenditure, adaptive thermogenesis, and adipose tissue lipolysis via decreased sympathetic tone (Quarta et al., 2010). Given our observations that ABHD6 disruption in the VMH alters endocannabinoid-driven processes, we put mice on an HF diet. In spite of a similar food intake, VMH^{KO} mice were significantly heavier at the end of the 12-week protocol (+24%, $p < 0.01$) (Figures 4A and 4B). Feed efficiency was increased in VMH^{KO} mice ($p < 0.01$) (Figure 4C). Although there was no change in lean mass, fat mass was increased in VMH^{KO} mice (+16%, $p < 0.05$) (Figure 4D). More specifically, the subcutaneous inguinal fat depot was significantly heavier in VMH^{KO} animals (+34%, $p < 0.05$), whereas no significant change was detected in the epididymal fat depot (Figure 4E). Interscapular brown fat mass of VMH^{KO} mice was lighter than that of VMH^{WT} mice (−23%, $p < 0.05$) (Figure 4F). Glucose tolerance was similar between the groups (Figure S2F).

A switch from chow to HF feeding triggers a net increase in energy expenditure, an energy "wasting" homeostatic process referred to as adaptive thermogenesis. We found that after 12 weeks of HF diet, VMH^{KO} mice have reduced energy expenditure (normalized to metabolic mass) compared to VMH^{WT} mice during both the dark (−16%, $p < 0.05$) and light phases (−22%, $p < 0.01$) (Figures 4G and 4H). Compared to their chow-fed counterparts, VMH^{WT} mice on an HF diet showed a 40% increase in dark cycle energy expenditure, whereas VMH^{KO} mice exhibited a 21% increase (Figure 4I). No change was seen in RER (Figures S2C and S2D). Ambulatory activity of HF-fed VMH^{KO} was strongly reduced versus VMH^{WT} during the dark phase (−46%, $p < 0.05$) (Figures 4J and 4K). Although diminished locomotion could partly account for the reduced energy expenditure measured in the dark phase, no change in ambulatory activity was observed during the light phase, whereas energy expenditure remained lower. These results suggest that decreased

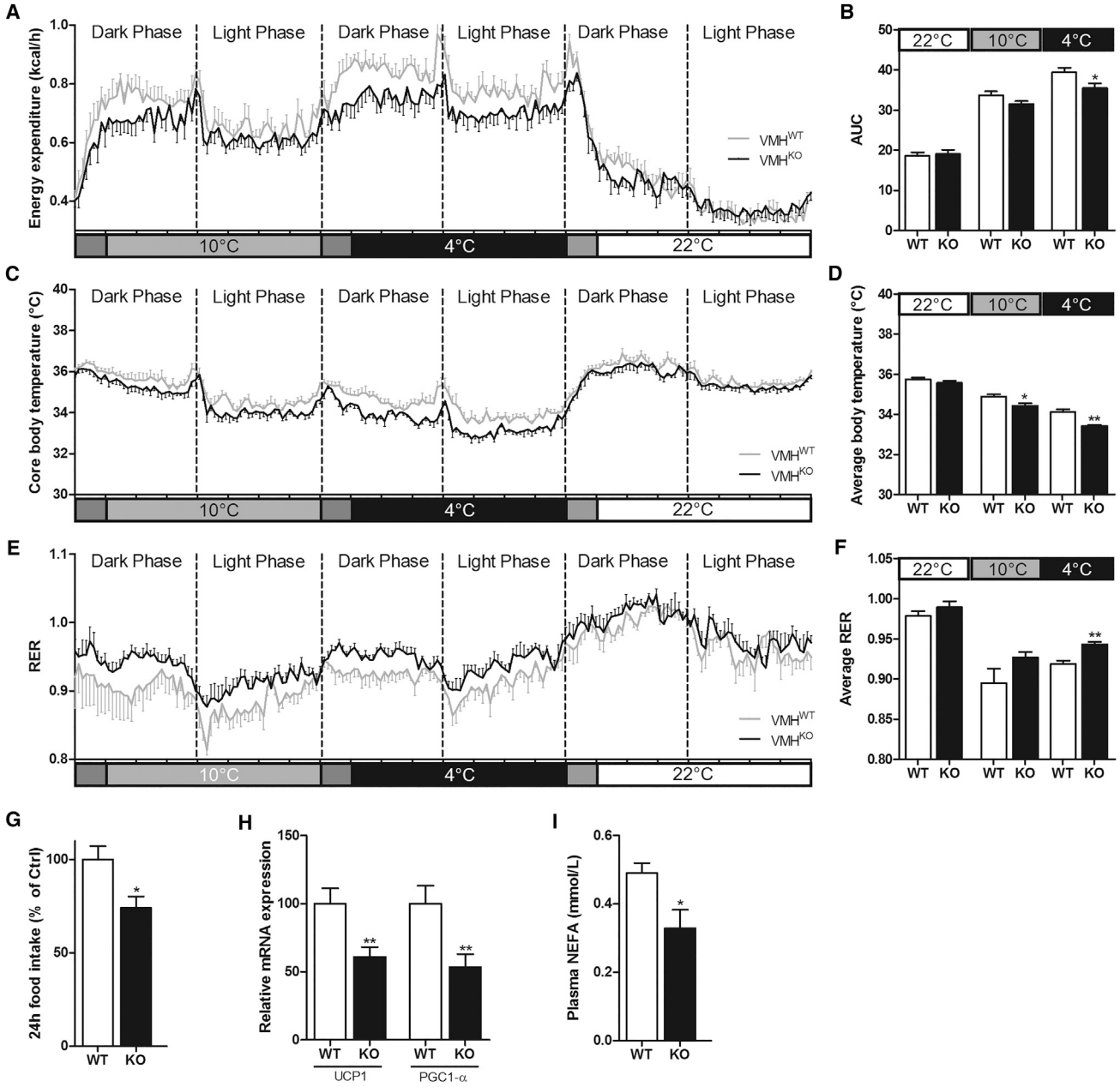

Figure 3. Impaired Cold-Induced Thermogenesis in VMH^{KO} Mice

(A) Energy expenditure over 72 hr at a different housing temperature (kcal/h).

(B) Area under the curve of combined dark and light phases for each temperature of (A) show reduced energy expenditure for VMH^{KO} mice at 10°C and 4°C. Data from the first 3 hr after temperature change were not used.

(C) Core body temperature over 72 hr at a different housing temperature (°C).

(D) Combined dark and light phases average body temperature of VMH^{KO} mice is reduced at 10°C and 4°C (from [C]). Data from the first 3 hr after temperature change were not used.

(E) RER over 72 hr at different housing temperature.

(F) Higher average RER of combined dark and light phase for each temperature of (E) in VMH^{KO} mice at 4°C. Data from the first 3 hr after temperature change were not used.

(G) Cumulative food intake over 24 hr at 4°C is decreased in VMH^{KO} mice. Food intake was corrected by body weight and normalized to % of control (VMH^{WT}).

(H) Decreased relative expression of mRNA markers of thermogenesis in brown adipose tissue of cold-exposed VMH^{KO} mice (corrected by *β-actin* and normalized to % of control).

(I) Plasma NEFAs are reduced in cold-exposed VMH^{KO} mice. All results are expressed as mean ± SEM, in which differences versus controls are expressed as *$p < 0.05$; **$p < 0.01$. n = 12 for (H). n = 6 per group for all other panels.

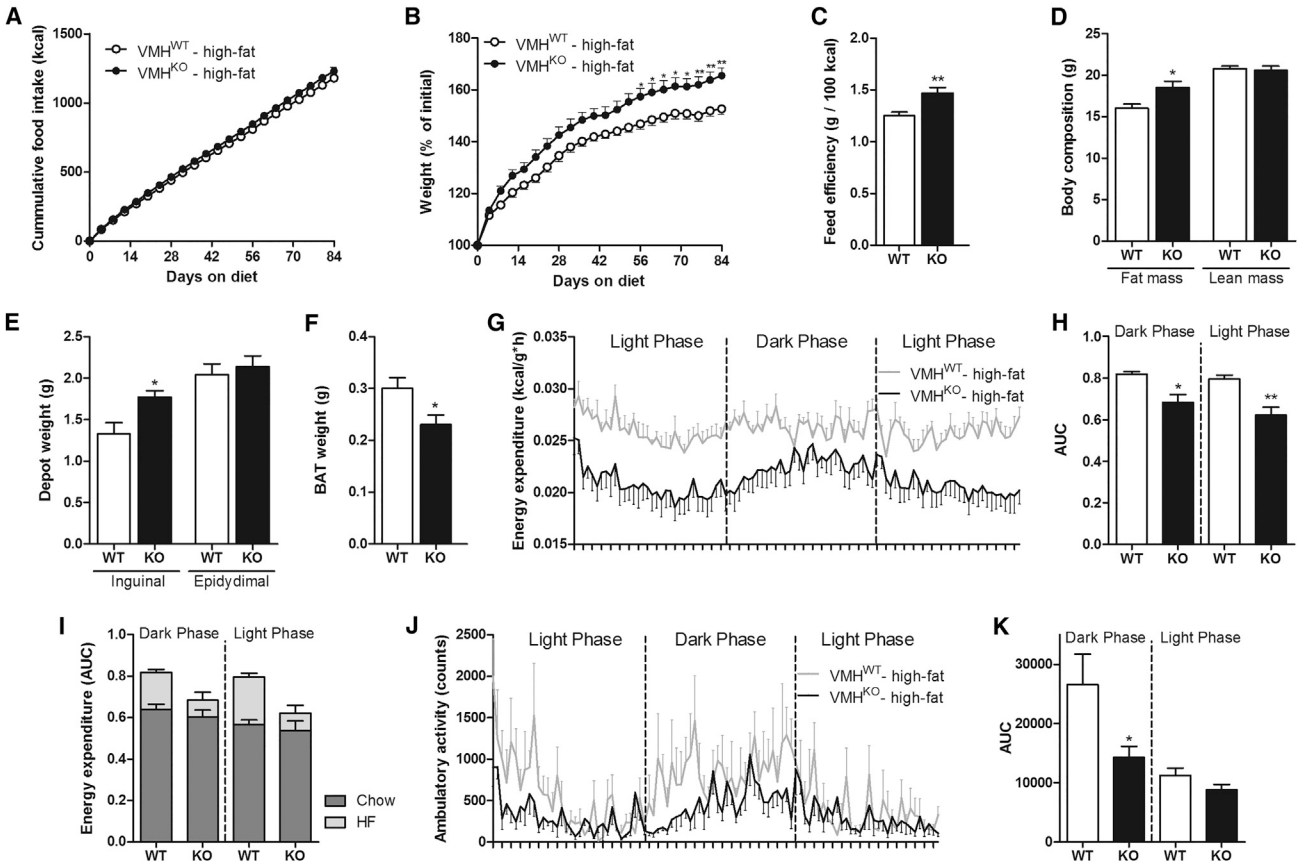

Figure 4. VMH^{KO} Mice Are Prone to Diet-Induced Obesity

(A) Cumulative high-fat food intake over 84 days (kcal).

(B) Body weight over 84 days of high-fat feeding is higher in VMH^{KO} mice (% of initial weight).

(C) Feed efficiency over 84 days is increased in VMH^{KO} mice.

(D) Increased fat mass in VMH^{KO} mice with unaltered lean mass (g).

(E) Heavier white inguinal and unchanged epididymal adipose tissue depot weight in VMH^{KO} mice (g).

(F) Brown adipose tissue (interscapular) depot weight is reduced in VMH^{KO} mice (g).

(G) Energy expenditure over 36 hr corrected by metabolic mass (kcal/g*h).

(H) Area under the curve of the last dark and light phase of (G) show decreased VMH^{KO} mice energy expenditure.

(I) Comparison of the energy expenditure of mice fed chow versus a high-fat diet, shown respectively in Figures 1E and 3H.

(J) Ambulatory activity over 36 hr (beam counts).

(K) Area under the curve of the last dark and light phase of (J) show decreased light phase activity in VMH^{KO} mice. All results are expressed as mean ± SEM, in which differences versus controls are expressed as *$p < 0.05$; **$p < 0.01$. n = 13 per group for (A–C). n = 7 per group for (D–F). n = 6 per group for (G, H, J, K). n = 5–7 per group for I.

locomotion is not the principle contributor to the reduced energy expenditure of knockout mice, but rather that these changes stem from a suppression in adaptive thermogenesis that is driven via sympathetic output.

Based on ABHD6 expression in the arcuate nucleus (ARC) (Figure S1A), a nucleus neighboring the VMH and playing a key role in energy balance, we tested if ARC ABHD6 influences diet-induced obesity (DIO) using a similar Cre-viral approach. The disruption of ABHD6 in ARC neurons did not affect food intake, body weight, energy expenditure, and locomotor activity in animals fed with chow or a high-fat diet (Figures S3A–S3H). In contrast to the VMH, ABHD6 disruption in the ARC did not alter the susceptibility to DIO and thus supports the specificity of our VMH^{KO} model.

Resistance to Diet-Induced Weight Loss in VMH^{KO} Mice

The maladaptive thermogenic response of VMH^{KO} mice to an HF diet enhances sensitivity to diet-induced obesity. To further evaluate the capacity to adapt to changing energy demands, a new cohort of VMH^{KO} and VMH^{WT} mice was transitioned (D0) to chow after a 12-week HF regimen. We followed body weight, energy expenditure, RER, ambulatory activity, and food intake for their last 7 days on an HF diet (D-7 to D0) and the following 35 days on chow (D0 to D+35), as schematized in Figure 5A. From D-7 to D+35, VMH^{WT} mice lost an average of 2.9 g (6% of their body weight) during the first 14 days of diet transition, and then their body weights started to plateau (Figures 5B–5D). VMH^{KO} mice, on the other hand, lost an average of 0.4 g (< 1% of their body weight) ($p < 0.01$). While on HF diet, VMH^{WT}

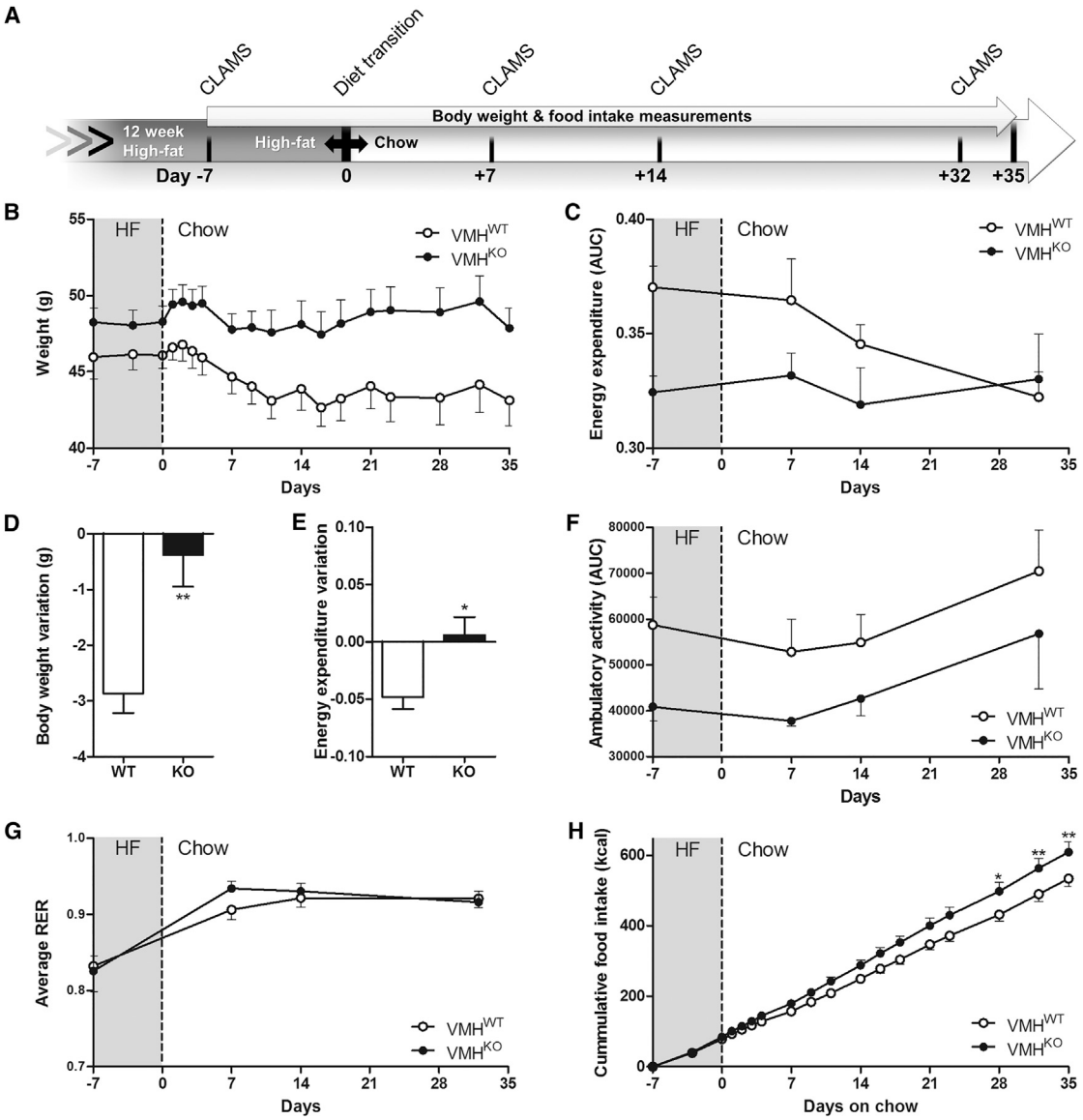

Figure 5. Energy Metabolism Flexibility Is Altered in VMH^{KO} Mice

(A) Timeline of diet transition protocol.

(B) Body weight from D-7 to D+35 (g).

(C) Area under the curve of combined dark and light phase energy expenditure corrected by body weight does not change during diet transition in VMH^{KO} mice.

(D) VMH^{KO} mice do not lose body weight from D-7 to D+35 (g).

(E) Energy expenditure variation from D-7 to D+32 is null in VMH^{KO} mice.

(F) Ambulatory activity variation from D-7 to D+32.

(G) RER variation from D-7 to D+32.

(H) Cumulative food intake from D-7 to D+35 (kcal) is higher in VMH^{KO} mice. All results are expressed as mean ± SEM, in which differences versus controls are expressed as *$p < 0.05$; **$p < 0.01$. n = 6 per group.

mice at D-7 had a higher energy expenditure than VMH^{KO} mice did (Figure 5C), reproducing the results previously obtained in Figure 3H. They showed a decrease of energy expenditure from D-7 to D+32 (−13%), mostly after D+7, and thereby defended body weight in response to transition to chow (Figures 5C–5E). VMH^{KO} energy expenditure was, in contrast, stable throughout D-7 to D+35. Energy expenditure variation from D-7 to D+35 was hence different between the groups ($p < 0.05$) (Figure 5E). Ambulatory activity was slightly lower in VMH^{KO} throughout the protocol (Figure 5F), as previously shown in both chow- and HF-fed cohorts (Figures 2G and 4J). The difference between the groups in ambulatory activity did not vary over time and thus should not explain the changes in energy expenditure between VMH^{KO} and VMH^{WT} mice. Expectedly,

the average RER for both groups increased following the diet transition, which is representative of reduced lipid utilization, and there were no differences between the groups (Figure 5G). Although cumulative food intake for the HF feeding period was similar between the two groups, VMH^{KO} mice consumed more food than controls did toward the end of the chow-feeding protocol (D+35, +15%, $p < 0.01$), contributing to the absence of weight loss (Figure 5H).

By simultaneously inspecting food intake, body weight, and calorimetric data at specific time points during the diet transition study, we can infer that most of the weight loss achieved by VMH^{WT} mice occurred at the beginning of diet transition, during a period in which adaptive thermogenesis is still considerably active. The absence of weight loss immediately following transition to chow in VMH^{KO} mice is thus explained via the lack of adaptive thermogenesis, as we have documented. Together with the HF-feeding study, these results imply that the disruption of ABHD6 in neurons of the VMH dampens the ability of mice to adapt energy homeostasis (food intake and energy expenditure) according to diet composition, increasing their susceptibility to diet-induced obesity and resistance to dieting-induced weight loss.

Conclusion

Energy metabolism is transformative to environmental conditions. This flexible nature of metabolism is largely adaptive for the organism. The leading exception is humans with access to plenty of food and little necessity to engage in physical activity to procure food, for which metabolism can be problematically inflexible to a shifting diet and exercise lifestyle (e.g., resting energy expenditure; Fothergill et al., 2016). The capacity of endocannabinoids to actively fine tune neuronal activity is well-suited to the central mechanisms underlying adjustments of energy metabolism. In this study, we demonstrate that increasing intrinsic 2-AG levels in the VMH by removing the lipase responsible for its postsynaptic degradation significantly blunts the counter-regulatory response to fasting, cold exposure, nutrient excess, and dieting.

In conditions of freely available chow and ambient temperatures, the absence of ABHD6 in neurons of the VMH had little effect on energy balance; however, metabolic challenges that potentiate 2-AG accumulation hindered homeostatic responses. In agreement with the demonstration that ABHD6 regulates stimulus-dependent accumulation of 2-AG in primary neurons and that ABHD6 contribution to total 2-AG degradation is relatively modest under basal conditions (Marrs et al., 2010), our finding that VMH 2-AG levels were unchanged in fed conditions, while elevated in knockout mice following fasting, is not surprising. Collectively, our results suggest that ABHD6 is a regulatory gatekeeper of 2-AG pools in the face of challenges that stimulate the ECS. Whether or not the effects of VMH ABHD6 neuronal deletion and high 2-AG levels are mediated in part by CB1R desensitization or alternate mechanisms is unknown. Of note, mice deficient for CB1R in glutamatergic neurons of the brain, which define the vast majority of VMH neurons (Ziegler et al., 2002), are also hypophagic only after food deprivation (Bellocchio et al., 2010). In addition, CB1R deletion in SF1-positive VMH neurons or throughout the whole hypothalamus regulates "metabolic flexibility" by hindering energy expenditure upon transition to a high-fat diet (Cardinal et al., 2014).

ABHD6 loss of function in the whole body or in peripheral metabolic tissues has recently been noted for having protective actions against DIO (Thomas et al., 2013; Zhao et al., 2016). Contributing to a catabolic phenotype, pan-ABHD6 knockout mice exhibit a greater energy expenditure, which is proposed to be due to direct actions of ABHD6 in brown adipose tissue (Zhao et al., 2016). It is clear that removal of ABHD6 function in the VMH has different actions that are in line with the function of this nucleus. By showing that absence of ABHD6 in VMH neurons attenuates adaptive thermogenesis, our findings provide mechanistic insights on SNS-dependent regulation of thermogenesis by 2-AG accumulation in the VMH. Because these results highlight VMH neuronal ABHD6 and 2-AG as a major influence on energy metabolism flexibility, they suggest exploring ways to target the endocannabinoid system in the VMH as a therapeutic means to alter energy metabolism.

EXPERIMENTAL PROCEDURES

Animals

All protocols were approved by the CRCHUM animal care committee and were conducted in accordance with the guidelines of the Canadian Council on Animal Care. Our group generated $ABHD6^{lox/lox}$ mice (backcrossed to C57BL/6N), as previously described (Zhao et al., 2014). Male mice were individually housed under a reverse cycle in environmentally controlled rooms (22°C–24°C), with ad libitum access to food. All testing and sacrifices were carried out during the dark phase. All mice were sacrificed under isoflurane anesthesia, and brain, plasma, brown, and white adipose tissue depots were harvested and frozen.

In Vivo Metabolic Assessments

Mice were fed standard chow or an HF diet (modified AIN-93G purified rodent diet with 50% kcal from fat derived from palm oil; Hryhorczuk et al., 2016). Body weight and food intake were measured twice weekly. Lean and fat mass were assessed by nuclear echo MRI. Oxygen consumption (VO_2), carbon dioxide production (VCO_2) for indirect calorimetry, and ambulatory movement were measured after a 24-hr habituation period in a Comprehensive Lab Animal Monitoring System (CLAMS) at 22°C (Colombus Instruments). For cold-exposure studies, sterile temperature probes (G2 HR E-mitter, Bio-Lynx) were implanted intraperitoneally (i.p.) 2 weeks prior to the experiment. After complete recovery, core body temperature was recorded using indirect calorimetry, in addition to the other parameters, for a period of 96 hr under different temperature settings (24-hr habituation at 22°C, 24 hr at 10°C, 24 hr at 4°C, and 24 hr at 22°C). Energy expenditure was calculated by multiplying the VO_2 value by $(3.815 + 1.232 \times VCO_2/VO_2)$, and corrected by metabolic mass (lean mass + 0.2 fat mass; Even and Nadkarni, 2012) when echo MRI data were available.

Feeding Experiments

Mice were habituated to handling. For fasting-refeeding studies, mice were fasted for 0, 2, or 4 hr (starting 1 hr before the onset of the dark phase) or 18 hr. Food intake was measured at the beginning of the dark cycle for 2 hr. When indicated, the CB1R agonist WIN55-212 or vehicle was injected i.p. right before refeeding. For WWL70 and orlistat (pan-lipase inhibitor) studies, animals were fasted for 4 hr (starting 1 hr before the onset of the dark phase). One hr later, animals received intra-VMH infusion of orlistat (1.25 μg), WWL70 (1.0 μg), or vehicle in 500 nL. Food pellets were put in the cages 3 hr later, and 1-hr food intake was measured. Each feeding experiment was performed using a within-subject design, in which all animals received the treatments and corresponding vehicle in a counterbalanced order, with at least 1 week of recovery in between the experiments. Food intake for

fasting-refeeding experiments was corrected by body weight and normalized to average VMH^{WT} consumption on control treatment.

Statistical Analysis

Results are expressed as mean ± SEM. Groups were compared using one-way or two-way ANOVA, with Bonferroni post hoc tests, t tests, or linear regression, as indicated using Prism 5.0 software (GraphPad). Statistical significance was set as $p < 0.05$, where $^{*}p < 0.05$, $^{**}p < 0.01$, and $^{***}p < 0.001$.

For methods related to stereotaxic surgeries and VMH cannulation, VMH 2-AG levels, elevated plus maze test, real-time qPCR, and glucose tolerance test, see the Supplemental Experimental Procedures.

SUPPLEMENTAL INFORMATION

Supplemental Information includes Supplemental Experimental Procedures and three figures and can be found with this article online at http://dx.doi.org/10.1016/j.celrep.2016.10.004.

AUTHOR CONTRIBUTIONS

S.F. and T.A. contributed equally to the intellectual and financial aspects of the study. A.F., S.F., and T.A. designed the study, were involved in the analysis, and co-wrote the manuscript. A.F., S.T., L.D.S., and K.B. performed the experiments. S.R.M.M. and M.P. provided the $ABHD6^{lox/lox}$ mouse strain. M.-L.P. performed the 2-arachidonoyl-glycerol measurements. All authors were involved in the continuous critical analysis of data and contributed to the manuscript edition.

ACKNOWLEDGMENTS

This work was supported by Canadian Institutes of Health Research (CIHR) grants to T.A. (MOP115042) and to S.F. (MOP123280), a grant from Montreal Diabetes Research Center-Diabète Québec to S.F., and a CIHR grant to M.P. and S.R.M.M. (MOP114974). A.F. holds a Canadian Diabetes Association postdoctoral fellowship. S.T. and K.B. were supported by fellowships from Diabète Québec, and L.D.S. was supported by a Fonds de Recherche Québec Santé (FRQS) doctoral fellowship. T.A. was supported by a salary award from FRQS, and S.F. was supported by a New Investigator salary award from CIHR. M.P. holds the Canada Research Chair in Diabetes and Metabolism. We thank Demetra Rodaros for technical help and the Metabolic Phenotyping Core and Metabolomics Core of CRCHUM and Montreal Diabetes Research Center for their services.

Received: May 19, 2016
Revised: August 30, 2016
Accepted: September 30, 2016
Published: October 25, 2016

REFERENCES

Bellocchio, L., Lafenêtre, P., Cannich, A., Cota, D., Puente, N., Grandes, P., Chaouloff, F., Piazza, P.V., and Marsicano, G. (2010). Bimodal control of stimulated food intake by the endocannabinoid system. Nat. Neurosci. *13*, 281–283.

Blankman, J.L., Simon, G.M., and Cravatt, B.F. (2007). A comprehensive profile of brain enzymes that hydrolyze the endocannabinoid 2-arachidonoylglycerol. Chem. Biol. *14*, 1347–1356.

Busquets-Garcia, A., Desprez, T., Metna-Laurent, M., Bellocchio, L., Marsicano, G., and Soria-Gomez, E. (2015). Dissecting the cannabinergic control of behavior: the where matters. Bioessays *37*, 1215–1225.

Cardinal, P., André, C., Quarta, C., Bellocchio, L., Clark, S., Elie, M., Leste-Lasserre, T., Maitre, M., Gonzales, D., Cannich, A., et al. (2014). CB1 cannabinoid receptor in SF1-expressing neurons of the ventromedial hypothalamus determines metabolic responses to diet and leptin. Mol. Metab. *3*, 705–716.

Di Marzo, V., Goparaju, S.K., Wang, L., Liu, J., Bátkai, S., Járai, Z., Fezza, F., Miura, G.I., Palmiter, R.D., Sugiura, T., et al. (2001). Leptin-regulated endocannabinoids are involved in maintaining food intake. Nature *410*, 822–825.

Even, P.C., and Nadkarni, N.A. (2012). Indirect calorimetry in laboratory mice and rats: principles, practical considerations, interpretation and perspectives. Am. J. Physiol. Regul. Integr. Comp. Physiol. *303*, R459–R476.

Fothergill, E., Guo, J., Howard, L., Kerns, J.C., Knuth, N.D., Brychta, R., Chen, K.Y., Skarulis, M.C., Walter, M., Walter, P.J., et al. (2016). Persistent metabolic adaptation 6 years after "The Biggest Loser" competition. Obesity (Silver Spring) *24*, 1612–1619.

Hanus, L., Avraham, Y., Ben-Shushan, D., Zolotarev, O., Berry, E.M., and Mechoulam, R. (2003). Short-term fasting and prolonged semistarvation have opposite effects on 2-AG levels in mouse brain. Brain Res. *983*, 144–151.

Higuchi, S., Irie, K., Yamaguchi, R., Katsuki, M., Araki, M., Ohji, M., Hayakawa, K., Mishima, S., Akitake, Y., Matsuyama, K., et al. (2012). Hypothalamic 2-arachidonoylglycerol regulates multistage process of high-fat diet preferences. PLoS ONE *7*, e38609.

Holtzman, D., Lovell, R.A., Jaffe, J.H., and Freedman, D.X. (1969). 1-delta9-tetrahydrocannabinol: neurochemical and behavioral effects in the mouse. Science *163*, 1464–1467.

Hryhorczuk, C., Florea, M., Rodaros, D., Poirier, I., Daneault, C., Des Rosiers, C., Arvanitogiannis, A., Alquier, T., and Fulton, S. (2016). Dampened mesolimbic dopamine function and signaling by saturated but not monounsaturated dietary lipids. Neuropsychopharmacology *41*, 811–821.

Kim, K.W., Zhao, L., Donato, J., Jr., Kohno, D., Xu, Y., Elias, C.F., Lee, C., Parker, K.L., and Elmquist, J.K. (2011). Steroidogenic factor 1 directs programs regulating diet-induced thermogenesis and leptin action in the ventral medial hypothalamic nucleus. Proc. Natl. Acad. Sci. USA *108*, 10673–10678.

Kirkham, T.C., Williams, C.M., Fezza, F., and Di Marzo, V. (2002). Endocannabinoid levels in rat limbic forebrain and hypothalamus in relation to fasting, feeding and satiation: stimulation of eating by 2-arachidonoyl glycerol. Br. J. Pharmacol. *136*, 550–557.

Koch, M., Varela, L., Kim, J.G., Kim, J.D.J.G., Hernández-Nuño, F., Simonds, S.E., Castorena, C.M., Vianna, C.R., Elmquist, J.K., Morozov, Y.M., et al. (2015). Hypothalamic POMC neurons promote cannabinoid-induced feeding. Nature *519*, 45–50.

Marrs, W.R., Blankman, J.L., Horne, E.A., Thomazeau, A., Lin, Y.H., Coy, J., Bodor, A.L., Muccioli, G.G., Hu, S.S., Woodruff, G., et al. (2010). The serine hydrolase ABHD6 controls the accumulation and efficacy of 2-AG at cannabinoid receptors. Nat. Neurosci. *13*, 951–957.

Marsicano, G., and Lutz, B. (1999). Expression of the cannabinoid receptor CB1 in distinct neuronal subpopulations in the adult mouse forebrain. Eur. J. Neurosci. *11*, 4213–4225.

Nass, S.R., Long, J.Z., Schlosburg, J.E., Cravatt, B.F., Lichtman, A.H., and Kinsey, S.G. (2015). Endocannabinoid catabolic enzymes play differential roles in thermal homeostasis in response to environmental or immune challenge. J. Neuroimmune Pharmacol. *10*, 364–370.

Naydenov, A.V., Horne, E.A., Cheah, C.S., Swinney, K., Hsu, K.-L., Cao, J.K., Marrs, W.R., Blankman, J.L., Tu, S., Cherry, A.E., et al. (2014). ABHD6 blockade exerts antiepileptic activity in PTZ-induced seizures and in spontaneous seizures in R6/2 mice. Neuron *83*, 361–371.

Quarta, C., Bellocchio, L., Mancini, G., Mazza, R., Cervino, C., Braulke, L.J., Fekete, C., Latorre, R., Nanni, C., Bucci, M., et al. (2010). CB(1) signaling in forebrain and sympathetic neurons is a key determinant of endocannabinoid actions on energy balance. Cell Metab. *11*, 273–285.

Thomas, G., Betters, J.L., Lord, C.C., Brown, A.L., Marshall, S., Ferguson, D., Sawyer, J., Davis, M.A., Melchior, J.T., Blume, L.C., et al. (2013). The serine hydrolase ABHD6 is a critical regulator of the metabolic syndrome. Cell Rep. *5*, 508–520.

Wen, J., Ribeiro, R., Tanaka, M., and Zhang, Y. (2015). Activation of CB2 receptor is required for the therapeutic effect of ABHD6 inhibition in experimental autoimmune encephalomyelitis. Neuropharmacology *99*, 196–209.

Zhao, S., Mugabo, Y., Iglesias, J., Xie, L., Delghingaro-Augusto, V., Lussier, R., Peyot, M.-L., Joly, E., Taïb, B., Davis, M.A., et al. (2014). α/β-Hydrolase domain-6-accessible monoacylglycerol controls glucose-stimulated insulin secretion. Cell Metab. *19*, 993–1007.

Zhao, S., Poursharifi, P., Mugabo, Y., Levens, E.J., Vivot, K., Attane, C., Iglesias, J., Peyot, M.L., Joly, E., Madiraju, S.R., et al. (2015). α/β-Hydrolase domain-6 and saturated long chain monoacylglycerol regulate insulin secretion promoted by both fuel and non-fuel stimuli. Mol. Metab. *4*, 940–950.

Zhao, S., Mugabo, Y., Ballentine, G., Attane, C., Iglesias, J., Poursharifi, P., Zhang, D., Nguyen, T.A., Erb, H., Prentki, R., et al. (2016). α/β-Hydrolase domain 6 deletion induces adipose browning and prevents obesity and type 2 diabetes. Cell Rep. *14*, 2872–2888.

Ziegler, D.R., Cullinan, W.E., and Herman, J.P. (2002). Distribution of vesicular glutamate transporter mRNA in rat hypothalamus. J. Comp. Neurol. *448*, 217–229.